

Research Article

The Design of LQG Controller for Active Suspension Based on Analytic Hierarchy Process

Lingjiang Chai and Tao Sun

*Institute of Automotive Engineering, College of Mechanical Engineering,
University of Shanghai for Science and Technology, Shanghai 200093, China*

Correspondence should be addressed to Lingjiang Chai, chailingjiang@163.com and Tao Sun, tao_sun531@163.com

Received 19 October 2009; Revised 9 March 2010; Accepted 23 April 2010

Academic Editor: Jerzy Warminski

Copyright © 2010 L. Chai and T. Sun. This is an open access article distributed under the Creative Commons Attribution License, which permits unrestricted use, distribution, and reproduction in any medium, provided the original work is properly cited.

A full vehicle model with seven degrees of freedom based on active suspension control is established, and linear quadratic gaussian (LQG) is designed by applying optimal control theory. Especially, the methodology of Analytic Hierarchy Process (AHP) is used to make the selection of weighted coefficients of performance indexes, which can reduce ineffective job in contrast with experience method. From the simulation results, it is shown that ride quality of the vehicle with active suspension has been effectively improved in comparison with the vehicle of passive suspension by the methodology of AHP applying to the selection of the weights.

1. Introduction

Active suspension plays a major role for improving ride comfort of ground vehicle, which depends on its control algorithm design to a great extent, due to its effective isolation from road surface unevenness. Therefore, many experts have done researching for suspension control algorithms, such as optimal control theory, fuzzy control and neural net technology, and robust control [1–3]. Among them, optimal control theory is widely used, in which the linear quadratic gaussian control can ascertain weighted matrix of state variable and control variable by giving the optimal performance indexes. So the designer is offered an approach associated with weights selection of overall consideration of various factors of suspension system, to improve ride quality of ground vehicle.

The approach of selecting weighted coefficients is conventionally designed by experience, and results in a time-consuming and inefficient job. In [4, 5], it does not provide a method with the selection of weighting coefficients. In [6], AHP applying to the selection of the weights is only used in quarter vehicle model with 2 degrees of freedom (DOF), which

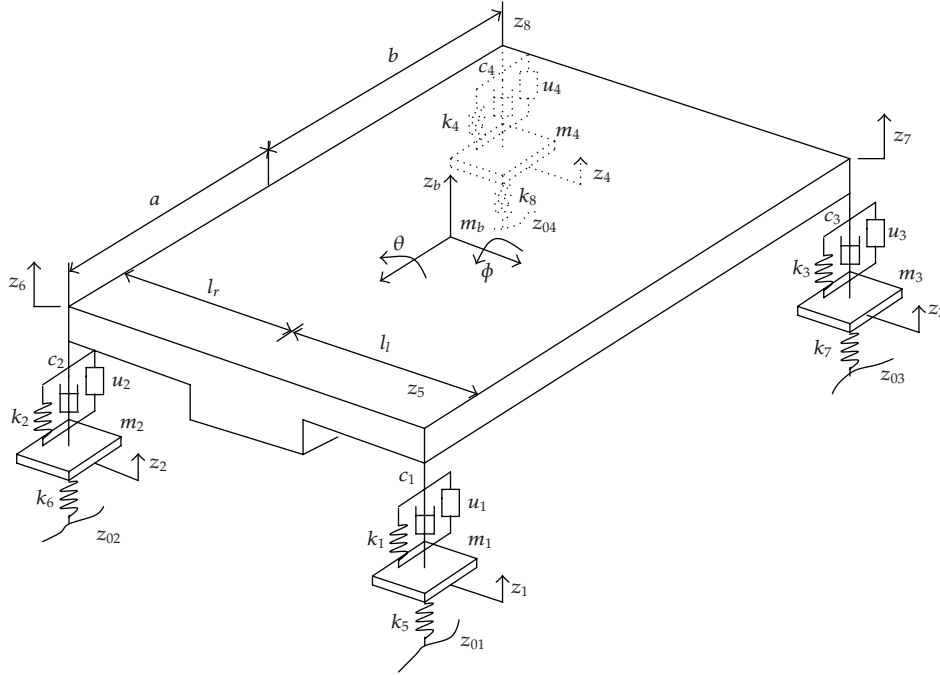


Figure 1: Model of completed vehicle with seven degrees freedom of suspension.

makes the limitations to design and analysis of vehicle performance. This paper makes use of AHP to optimize the weights of performance indexes in the design of active suspension LQG controller based on full vehicle model with 7 DOF. The simulation results illustrate that the body acceleration of active suspension has been effectively reduced, and ride quality of the vehicle has been improved by AHP applying to the selection of the weights.

2. Modeling of Active Suspension with 7 Degrees of Freedom

Building a dynamic model of vehicle suspension is the basis of system design and performance analysis. Quarter vehicle model with 2 DOF and half vehicle model with 4 DOF have limitations to design and analyze vehicle performance. In order to reflect vertical vibration of the vehicle, quarter vehicle model is often used to conceptual design of suspension and research of control theory. Half vehicle model can only reflect vertical and pitch vibration of the vehicle. Therefore, the completed vehicle model with 7 DOF in this paper is used to grasp comprehensive ride quality including body vertical jump, pitch and roll vibration of the vehicle. The model is shown in Figure 1.

The completed vehicle suspension itself is shown to consist of four springs k_1 , k_2 , k_3 , and k_4 , four dampers c_1 , c_2 , c_3 , and c_4 and four active forces actuator u_1 , u_2 , u_3 , and u_4 . The unsprung mass m_1 , m_2 , m_3 , and m_4 represent the equivalent mass due to the axle and tire. The vertical stiffness of the tires is represented by the springs k_5 , k_6 , k_7 , and k_8 . The variables z_1 , z_2 , z_3 , and z_4 represent the vertical displacements from static equilibrium of the unsprung mass. The variables z_5 , z_6 , z_7 , and z_8 represent the vertical displacements from static equilibrium of the sprung mass. The variables z_{01} , z_{02} , z_{03} , and z_{04} represent the

vertical displacements from static equilibrium of the road. z_b is vertical displacement of body mass. m_b is body mass. θ which encloses x -axis rotation is roll angle. ϕ which encloses y -axis rotation is pitch angle. The displacement from center of mass to front axle is a . The displacement from center of mass to rear axle is b . The displacement from center of mass to the center of left tire is l_l . The displacement from center of mass to the center of right tire is l_r .

The mathematical model is set up as follows:

$$\begin{aligned}
m_b \ddot{z}_b &= c_1(\dot{z}_1 - \dot{z}_5) + k_1(z_1 - z_5) + u_1 + c_2(\dot{z}_2 - \dot{z}_6) + k_2(z_2 - z_6) \\
&\quad + u_2 + c_3(\dot{z}_3 - \dot{z}_7) + k_3(z_3 - z_7) + u_3 + c_4(\dot{z}_4 - \dot{z}_8) + k_4(z_4 - z_8) + u_4, \\
I_P \ddot{\phi} &= [c_3(\dot{z}_3 - \dot{z}_7) + k_3(z_3 - z_7) + u_3 + c_4(\dot{z}_4 - \dot{z}_8) + k_4(z_4 - z_8) + u_4]b \\
&\quad - [c_1(\dot{z}_1 - \dot{z}_5) + k_1(z_1 - z_5) + u_1 + c_2(\dot{z}_2 - \dot{z}_6) + k_2(z_2 - z_6) + u_2]a, \\
I_r \ddot{\theta} &= [c_2(\dot{z}_2 - \dot{z}_6) + k_2(z_2 - z_6) + u_2 + c_4(\dot{z}_4 - \dot{z}_8) + k_4(z_4 - z_8) + u_4]l_r \\
&\quad - [c_1(\dot{z}_1 - \dot{z}_5) + k_1(z_1 - z_5) + u_1 + c_3(\dot{z}_3 - \dot{z}_7) + k_3(z_3 - z_7) + u_3]l_l, \\
m_1 \ddot{z}_1 &= k_5(z_{01} - z_1) + k_1(z_5 - z_1) + c_1(\dot{z}_5 - \dot{z}_1) - u_1, \\
m_2 \ddot{z}_2 &= k_6(z_{02} - z_2) + k_2(z_6 - z_2) + c_2(\dot{z}_6 - \dot{z}_2) - u_2, \\
m_3 \ddot{z}_3 &= k_7(z_{03} - z_3) + k_3(z_7 - z_3) + c_3(\dot{z}_7 - \dot{z}_3) - u_3, \\
m_4 \ddot{z}_4 &= k_8(z_{04} - z_4) + k_4(z_8 - z_4) + c_4(\dot{z}_8 - \dot{z}_4) - u_4.
\end{aligned} \tag{2.1}$$

When θ , ϕ is very small, the displacement equations of four end point with sprung mass are

$$\begin{aligned}
z_5 &= z_b + l_l \theta - a \phi, \\
z_6 &= z_b - l_r \theta - a \phi, \\
z_7 &= z_b + l_l \theta + b \phi, \\
z_8 &= z_b - l_r \theta + b \phi.
\end{aligned} \tag{2.2}$$

The road input model is the basis of automobile dynamic response and control. In general, the mathematical models of the road disturbances in time domain include random road disturbances model and discrete event road disturbances model. This paper will use them as road excitation input. There are four road inputs corresponding to left front tire, right front tire, left rear tire and right rear tire in this paper. So tread correlated of left and right tires and wheelbase lag of front and rear tires are considered. Based on these, random road input model [7] is built.

Firstly, the tread correlated equation of left and right tires is set up as follows:

$$\begin{aligned}
\begin{bmatrix} \dot{\eta}_{t1} \\ \dot{\eta}_{t2} \end{bmatrix} &= A_{\eta 1} \begin{bmatrix} \eta_{t1} \\ \eta_{t2} \end{bmatrix} + B_{\eta 1} W_1, \\
W_2 &= C_{\eta 1} \begin{bmatrix} \eta_{t1} \\ \eta_{t2} \end{bmatrix} + D_{\eta 1} W_1.
\end{aligned} \tag{2.3}$$

Secondly, the wheelbase lag equation of front and rear tires is set up and second-order Pade approximation algorithm is used to express time delay. So the model is

$$\begin{bmatrix} \dot{\eta}_{t3} \\ \dot{\eta}_{t4} \end{bmatrix} = \begin{bmatrix} -\frac{6}{t} & -\frac{12}{t^2} \\ 1 & 0 \end{bmatrix} \begin{bmatrix} \eta_{t3} \\ \eta_{t4} \end{bmatrix} + \begin{bmatrix} \frac{12}{t^2} \\ 0 \end{bmatrix} W_1, \quad (2.4)$$

$$W_3 = [-t \ 0] \begin{bmatrix} \eta_{t3} \\ \eta_{t4} \end{bmatrix} + [0]W_1.$$

Lastly, a filtered white noise model of the four wheels random road inputs is

$$\begin{aligned} \dot{z}_0 &= F_w z_0 + B_{0\eta} \eta_t + B_0 W, \\ \dot{\eta}_t &= A_\eta \eta_t + B_\eta W, \end{aligned} \quad (2.5)$$

$z = [z_{01} \ z_{02} \ z_{03} \ z_{04}]^T$, $z_{01}, z_{02}, z_{03}, z_{04}$ represent road inputs of left front, right front, left rear, right rear tire, respectively. η_t is the state transition vector, $\eta_t = [\eta_{t1} \ \eta_{t2} \ \eta_{t3} \ \eta_{t4}]^T$. W is the white noise, $W = [W_1 \ W_2 \ W_3 \ W_4]^T$. t is time delay.

Besides random road profile, the model [8] of discrete event road disturbances is also set up as follows:

$$z = \begin{cases} -\frac{h}{2} \cos\left[\frac{2\pi vt}{x_l}\right] + \frac{h}{2}, & 0 \leq t \leq \frac{x_l}{v}, \\ 0, & t > \frac{x_l}{v}. \end{cases} \quad (2.6)$$

The length of arc road is x_l . The height from road surface to convex closure is h . v is velocity of vehicle running.

3. The Optimal Controller Design of Active Suspension

3.1. The State Equation of the System

For the completed vehicle model, the roll, pitch, jump vibration, suspension and tire deflection are very important performance items and should be chosen as output variables. So the state variables X^T , and output variables Y^T are shown as below:

$$\begin{aligned} X^T &= [z_b \ \dot{z}_b \ \theta \ \dot{\theta} \ \phi \ \dot{\phi} \ z_1 \ \dot{z}_1 \ z_2 \ \dot{z}_2 \ z_3 \ \dot{z}_3 \ z_4 \ \dot{z}_4], \\ Y^T &= [\dot{z}_b \ \ddot{\theta} \ \ddot{\phi} \ z_5 - z_1 \ z_6 - z_2 \ z_7 - z_3 \ z_8 - z_4 \ z_1 - z_{01} \ z_2 - z_{02} \ z_3 - z_{03} \ z_4 - z_{04}]. \end{aligned} \quad (3.1)$$

The state space model of the completed vehicle system can be written as

$$\begin{aligned} \dot{X} &= AX + Bu + Fz, \\ Y &= CX + Du. \end{aligned} \quad (3.2)$$

In the above description, the state vector is denoted as X . u is the control vector. $u = [u_1 \ u_2 \ u_3 \ u_4]^T$. A is the system matrix. B is control matrix. F is disturbance matrix. C is the output matrix. D is transfer matrix.

3.2. The LQG Controller Design

The aim of optimal control of active suspension is to improve ride comfort and handling stability. The body acceleration, roll angle acceleration, pitch angle acceleration and tire deflection, therefore, should be depressed as much as possible. To avoid suspension bottoming, suspension working space is also limited. Considering the completed model is complex and has many trade-off performance items, the performance function is defined as follows:

$$\begin{aligned}
 J &= \frac{1}{2} \int_0^{\infty} \left[q_1 \ddot{z}_b^2 + q_2 \ddot{\theta}^2 + q_3 \ddot{\phi}^2 + q_4 (z_5 - z_1)^2 + q_5 (z_6 - z_2)^2 \right. \\
 &\quad + q_6 (z_7 - z_3)^2 + q_7 (z_8 - z_4)^2 + q_8 (z_1 - z_{01})^2 + q_9 (z_2 - z_{02})^2 \\
 &\quad \left. + q_{10} (z_3 - z_{03})^2 + q_{11} (z_4 - z_{04})^2 + r_1 u_1^2 + r_2 u_2^2 + r_3 u_3^2 + r_4 u_4^2 \right] dt \\
 &= \frac{1}{2} \int_0^{\infty} (Y^T Q Y + u^T R u) dt,
 \end{aligned} \tag{3.3}$$

q_1 is the weighted coefficient of body vertical acceleration. q_2 is the weighted coefficient of roll angle acceleration. q_3 is the weighted coefficient of pitch angle acceleration. $q_4, q_5, q_6,$ and q_7 are the weighted coefficients of suspension deflection. $q_8, q_9, q_{10},$ and q_{11} are the weighted coefficients of tire deflection. $r_1, r_2, r_3,$ and r_4 are the weighted coefficients of control vector. Q is the weight matrix of the state. R is the weight matrix of the control.

The formula (3.2) is substituted into formula (3.3), and the performance function is then written as

$$J = \frac{1}{2} \int_0^{\infty} \left[X^T \hat{Q} X + 2X^T N u + u^T \hat{R} u \right] dt. \tag{3.4}$$

There are $\hat{Q} = C^T Q C$, $N = C^T Q D$, and $\hat{R} = R + D^T Q D$ in formula (3.4).

The solution to the optimal control problem that minimizes this given performance index is a state feedback law $u = -KX$ where the feedback gain K is determined by solving the following Riccati equation:

$$\begin{aligned}
 AP + PA^T + Q - PBR^{-1}B^T P &= 0, \\
 K &= R^{-1} (N^T + B^T P).
 \end{aligned} \tag{3.5}$$

So the state equation of closed-loop is

$$\dot{X} = (A - BK)X + Fz. \tag{3.6}$$

3.3. The Selection of the Weights Based on AHP

AHP is a multicriteria decision aiding method based on a solid axiomatic foundation. It is a systematic procedure for dealing with complex decision making problems in which many competing alternatives exist. The procedure can be described as the following three steps [9].

(1) Making Pairwise Comparison

The evaluation matrices $H = (h_{ij})_{n \times n}$ are built up through pairwise comparing each decision factor under the topmost goal

$$H = (h_{ij})_{n \times n} = \begin{bmatrix} 1 & h_{12} & \cdots & \cdots & h_{1n} \\ \frac{1}{h_{12}} & 1 & h_{23} & \cdots & h_{2n} \\ \cdots & \frac{1}{h_{23}} & \cdots & \cdots & \cdots \\ \vdots & \vdots & & & \vdots \\ \frac{1}{h_{1n}} & \frac{1}{h_{2n}} & \cdots & \cdots & 1 \end{bmatrix}. \quad (3.7)$$

n is the number of factors.

The fundamental 1 to 9 scale can be used to rank the judgments as shown in Table 1. According to H matrices, the subject weights [6] are calculated as follows

(1) calculating H multiplying vector of every row

$$M = [M_1 \ M_2 \ \cdots \ M_n]^T, \quad (i, j = 1, 2, \dots, n), \quad (3.8)$$

$$M_i = \prod_{j=1}^n h_{ij},$$

(2) calculating $\sqrt[n]{M}$

$$\bar{E} = [\bar{E}_1 \ \bar{E}_2 \ \cdots \ \bar{E}_n]^T, \quad (i = 1, 2, \dots, n), \quad (3.9)$$

$$\bar{E}_i = \sqrt[n]{M_i},$$

(3) calculating positive vector of \bar{E}

$$E = \frac{\bar{E}_i}{\sum_{i=1}^n \bar{E}_i} \quad (i = 1, 2, \dots, n), \quad (3.10)$$

E is the subjective weighted coefficient of each evaluating index.

Table 1: A fundamental scale of 1 to 9.

i/j	Equally	Moderately	Strongly	Very	Extremely
h_{ij}	1	3	5	7	9

2, 4, 6, and 8 indicate the medium value of above pairwise comparison.

(2) Calculating Maximum Eigenvalue of Matrix H

$$\lambda_{\max} = \sum_{i=1}^n \frac{(HE)_i}{nE_i} \quad (i = 1, 2, \dots, n). \quad (3.11)$$

(3) Checking for Consistency

If every element in matrix H satisfies the equation $h_{ij} = 1/h_{ji}$ and $h_{ij} = h_{ik} \cdot h_{kj}$, the matrix H is the consistency matrix. The evaluation matrices are often not perfectly consistent due to people's random judgments. These judgment errors can be detected by a consistency ratio CR

$$CR = \frac{\lambda_{\max} - n}{RI(n - 1)} \quad (3.12)$$

RI is random index. When n is 11, RI equals 1.51. The value CR calculated is less than 1, the result is right. If CR is more than 1, the evaluation matrix needs to be revised on the basis of [10].

The formula fourteen has many weights which are calculated by AHP.

Firstly, according to the performance data of a passive antitype suspension under the given working condition, objective weights of evaluating indexes can be determined. Passive suspension to the specific demand for ride comfort under a given operation condition has σ . The objective weight of body acceleration is supposed to 1. According to [6], the equation of calculating other objective weights is

$$\sigma_a^2 \times 1 = \sigma^2 \times \beta. \quad (3.13)$$

Secondly, it needs to calculate subjective weighted proportion coefficient of evaluating indexes. The subjective weighted proportion coefficient of body vertical acceleration is supposed to be 1. The subjective weighted proportion coefficients of suspension and tire deflection are

$$E_1 = \frac{E_i}{r_i} \quad (i = 1, 2, \dots, n). \quad (3.14)$$

Lastly, the general weights of evaluating indexes of related to ride comfort can be obtained based on the objective weights and subjective weighted proportion coefficients

$$q = \beta \times \gamma. \quad (3.15)$$

Table 2: Parameter of a car.

Parameter	Value	Parameter	Value	Parameter	Value
a/m	1.3	$k_1, k_2, k_3, k_4/N/m$	20000	$I_p/kg \cdot m^2$	2440
b/m	1.5	$k_5, k_6, k_7, k_8/N/m$	200000	$I_r/kg \cdot m^2$	380
$l_l, l_r/m$	0.75	$c_1, c_2, c_3, c_4/N \cdot s/m$	1000		
m_b/kg	1380	$m_1, m_2, m_3, m_4/kg$	40		

Table 3: Comparison of RMS for the active and passive suspensions.

Index	Unit	RMS			
		$G_0 = 5 \times 10^{-6}$		$G_0 = 16 \times 10^{-6}$	
		active	passive	active	passive
\ddot{z}_b	m/s^2	1.172	1.342	1.6973	1.8356
$\ddot{\theta}$	rad/s^2	1.3002	1.5083	2.0746	2.4298
$\ddot{\phi}$	rad/s^2	0.86272	0.88079	1.3469	1.3609
$z_6 - z_2$	mm	12.97	16.898	20.28	23.031
$z_2 - z_{02}$	mm	2.3575	2.7589	3.7035	4.1664
$z_7 - z_3$	mm	20.35	22.549	27.136	27.752
$z_3 - z_{03}$	mm	6.8568	6.7861	10.914	10.714

The weights of the active suspension are derived as follows:

$$\begin{aligned}
 q_1 = 1, \quad q_2 \approx 1, \quad q_3 \approx 1, \quad q_4 = 1567, \quad q_5 = 1538 \\
 q_6 = 764, \quad q_7 = 305, \quad q_8 = 4279, \quad q_9 = 22821, \quad q_{10} = 2867, \quad q_{11} = 2423.
 \end{aligned} \tag{3.16}$$

4. Simulation Results and Analysis

The parameters [11] of a car are used in this paper as shown in Table 2. The velocity of the car is 20 m/s. The simulation time is 20 seconds in all. The road profile is a mixed random road excitation (smooth and rough) with the road roughness $G_0 = 5 \times 10^{-6}$ at the first 10 seconds, and 16×10^{-6} at the rest. The system simulation model of active suspension and passive suspension is built and simulated as in Table 2.

4.1. Root Mean Square (RMS) of the Active Suspension and Passive Suspension

From Table 3, it is shown that the active suspension with LQG controller reduces body acceleration and roll angle acceleration remarkably on two grade roads in contrast with the passive one. The RMS value of body acceleration of the active suspension on both grade roads reduces 13% and 8%, respectively. The RMS value of roll angle acceleration in two grade roads reduces 14% and 15%, respectively. But the pitch angle acceleration is not noticeable to depress. The simulation results also show that the RMS value of right front axle of the active suspension working space reduces 23% and 12%, respectively, on the two grade roads. But the RMS value of left rear axle working space reduces 10% and 2%, respectively. It is obviously that control effect for left rear axle working space is even worse than right front axle working

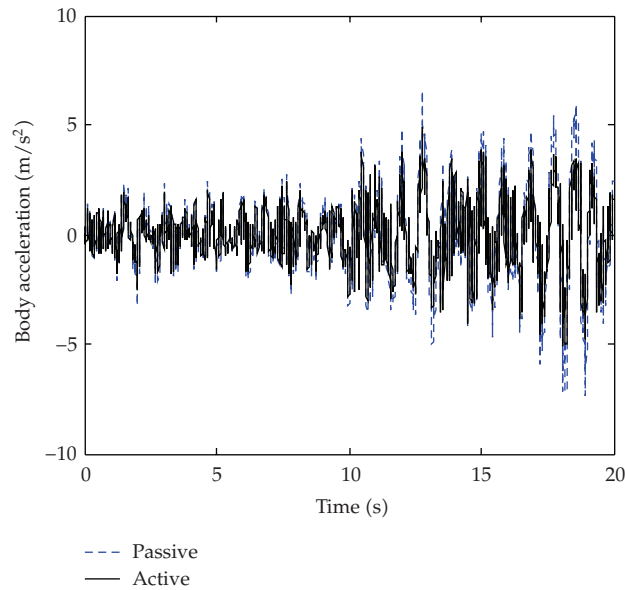


Figure 2: Body acceleration.

space. It can be seen that left rear wheel dynamic deflection of the passive suspension is better than that of the active suspension in Table 3, which shows that handling stability and ride comfort are incompatible to some extent.

4.2. Time Response of the Two Different Systems in Mixed Road Profile

From Figures 2 and 3, it can be seen that the active suspension with LQG controller remarkably reduces body acceleration and roll angle acceleration on both grade roads in contrast with the passive one. For Figures 4 and 5, it can be seen that the axles working space are controlled at the scope of the design requirements (± 100 mm). According to Gaussian characteristics of road profile distribution, the RMS of the largest suspension deflection is 33 mm. It is less than theoretical value and the design is reasonable. Compared to right front axle working space, the control effect of left rear axle working space is relatively worse. In addition, wheel dynamic deflection related to handling stability impacts the effect of tire and road adhesion. For Figures 6 and 7, the control has no effect on the left rear wheel dynamic deflection on two grade roads with comparison to the passive suspension, which results from the interaction and coupling of the indexes.

4.3. Time Response of the Two Different Systems in Random Road Excitation with Variations of Suspension Stiffness and Damping Parameters

Figures 8 and 9 are right front axle working space with suspension stiffness parameters decreasing 10 percent and increasing 10 percent, respectively. Figures 10 and 11 are right front axle working space with suspension damping coefficients decreasing 10 percent and

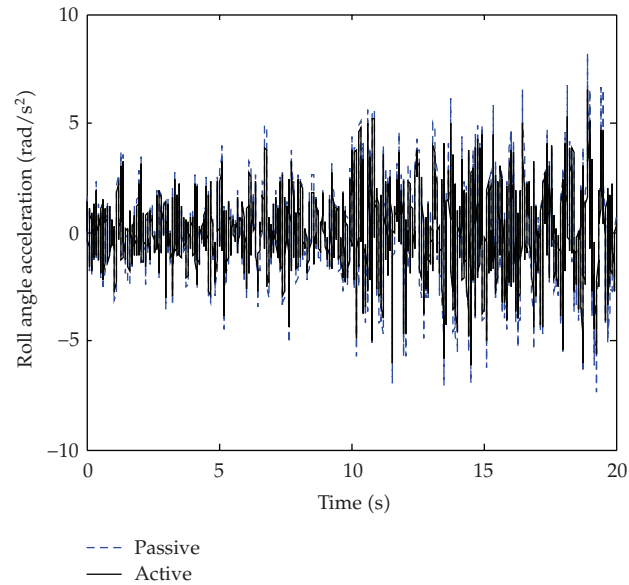


Figure 3: Roll angle acceleration.

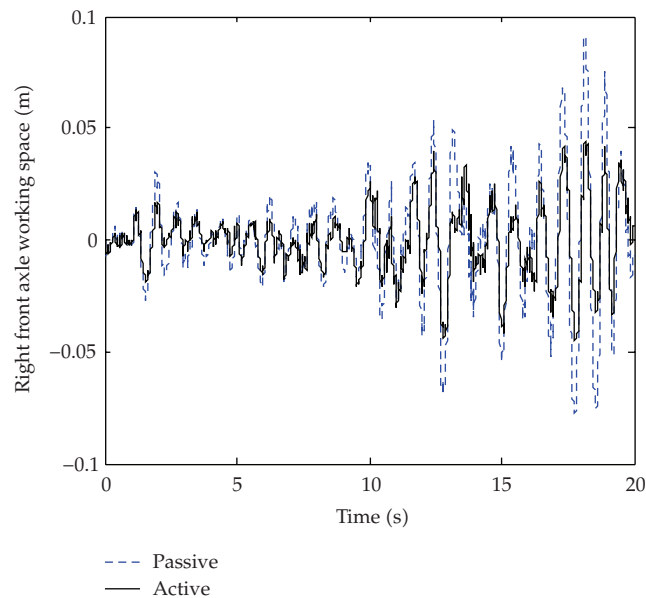


Figure 4: Right front axle working space.

increasing 10 percent, respectively. From Figures 8–11, it can be seen that active suspension control has shown a good effect at mixed road excitation in comparison with the passive suspension. It illustrates that LQG controller suspension system based on AHP has a good stability of performance when suspension stiffness and damping coefficients vary.

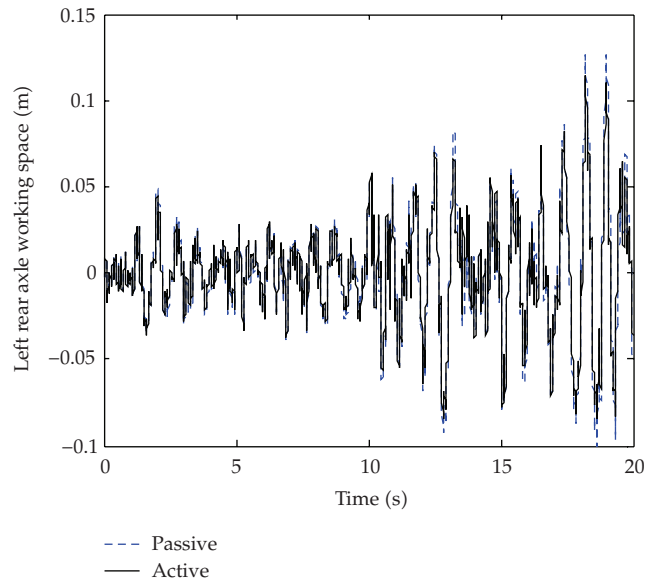


Figure 5: Left rear axle working space.

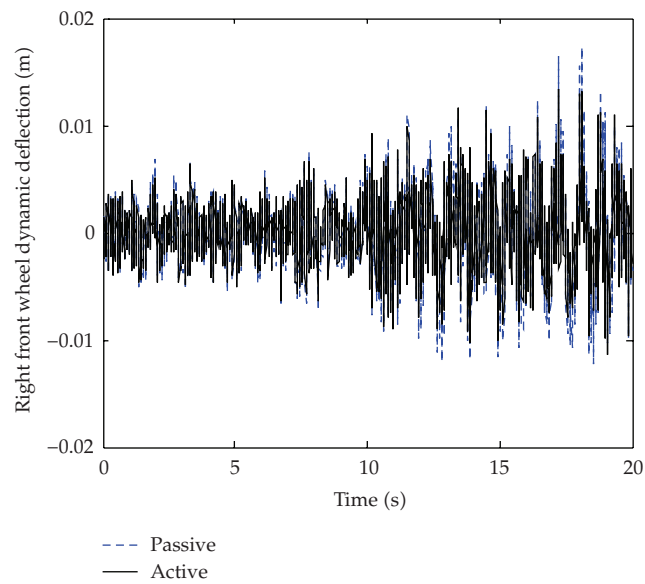


Figure 6: Right front wheel dynamic deflection.

4.4. Active Suspension Control Force at Mixed Random Road Excitation

It can be seen that, from Figures 12 and 13, suspension control force is within the control of actuator (± 1000 N). Under the effect of suspension control force, active suspension can effectively reduce to vibration transmission from uneven roads to the body of the vehicle.

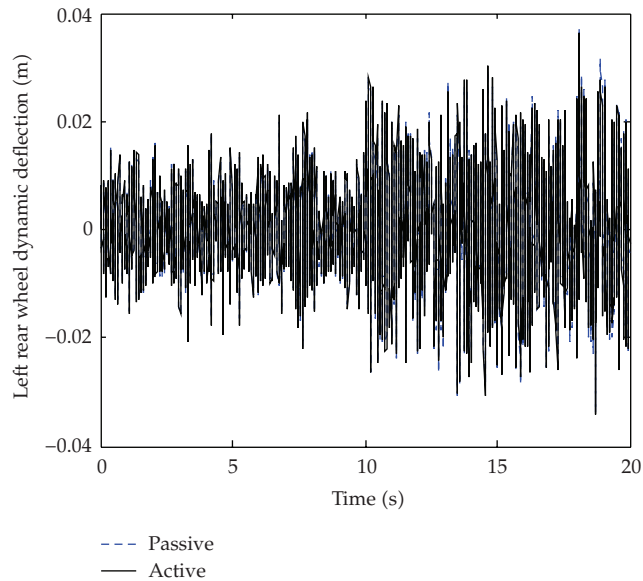


Figure 7: Left rear wheel dynamic deflection.

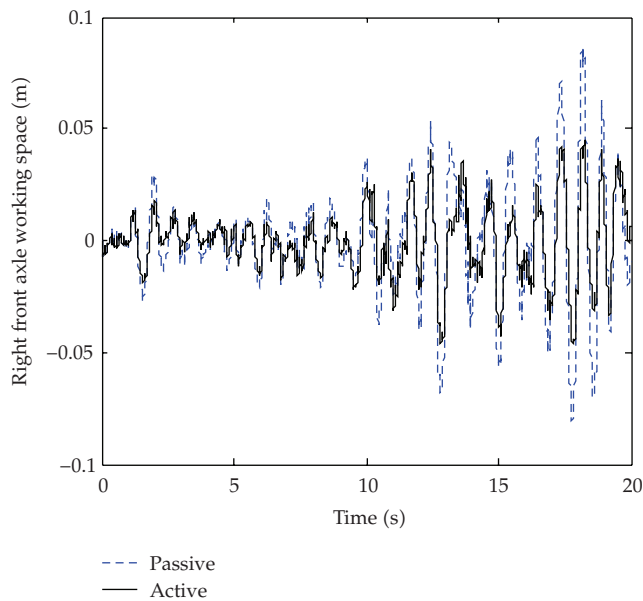


Figure 8: Right front axle working space (stiffness-18000).

Therefore, active suspension can availablely depress values of body acceleration, roll angle acceleration and so on in contrast with passive suspension. So the vehicle of active suspension can effectively improve ride comfort.

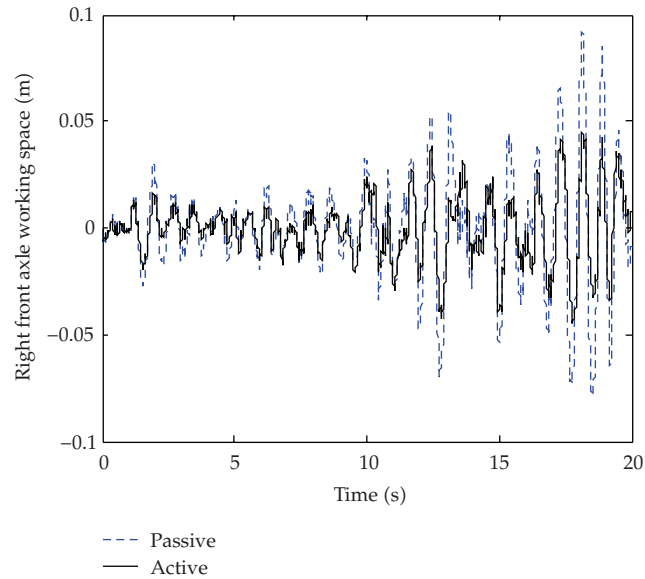


Figure 9: Right front axle working space (stiffness-22000).

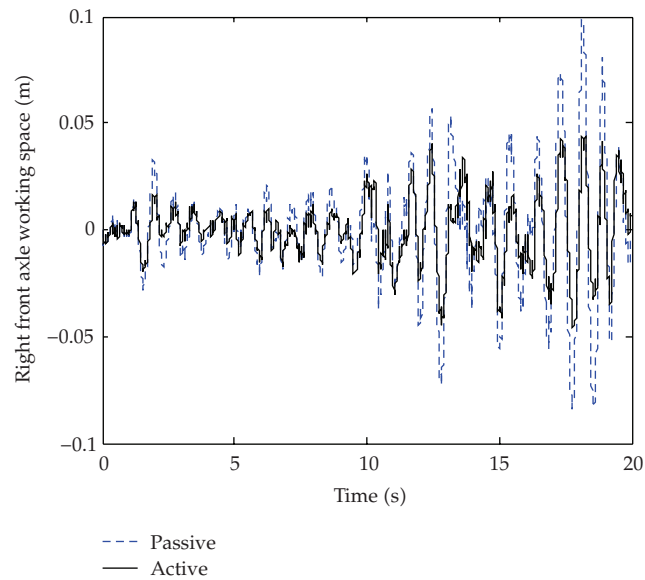


Figure 10: Right front axle working space (damping-900).

4.5. Power Spectral Density of the Two Different Systems in Conditions of the Same Road Roughness Coefficient (16×10^{-6})

From Figures 14, 15, and 16, it can be illustrated that vibration-isolation effect of active suspension is satisfactory at low frequency related to ride comfort of ground vehicle to a

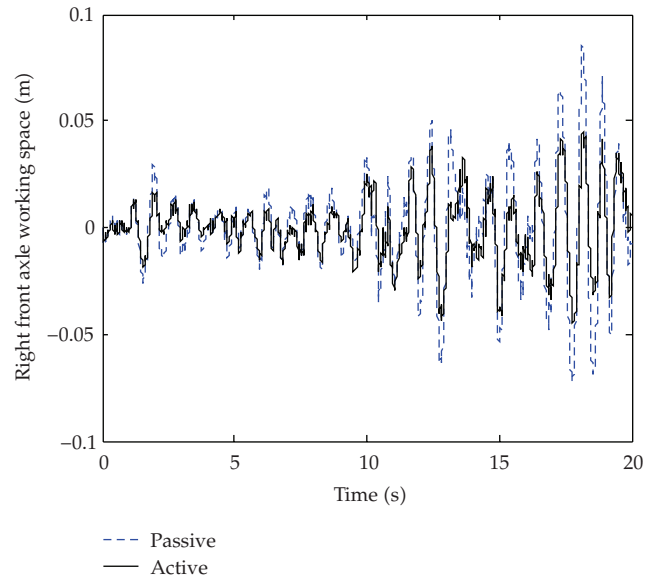


Figure 11: Right front axle working space (damping-1100).

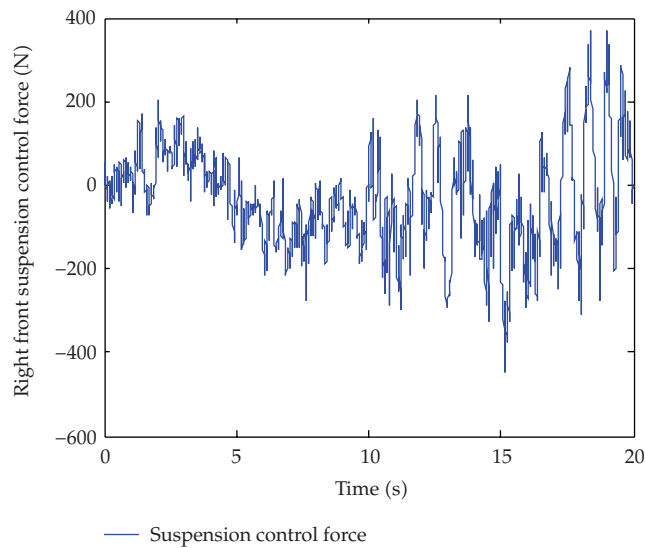


Figure 12: Right front suspension control force.

large extent, including body bounce vibration, roll and pitch mode and human sensitivity band. Meanwhile, the amplitudes near the tire resonance frequency associated with handling and stability of ground vehicle have no noticeable changes.

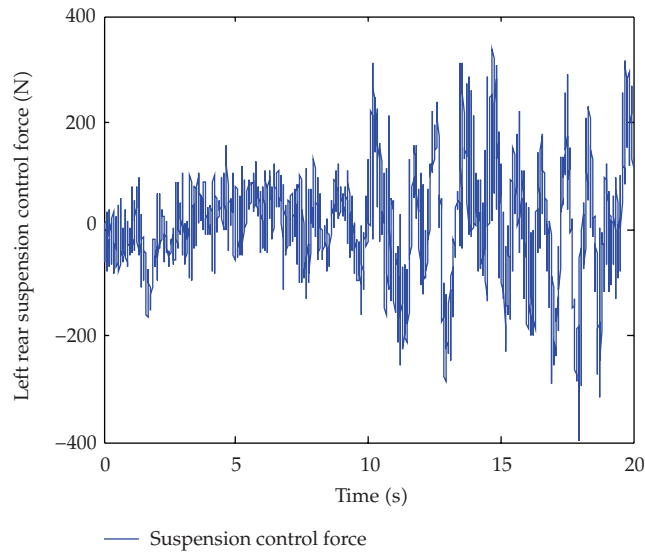


Figure 13: Left rear suspension control force.

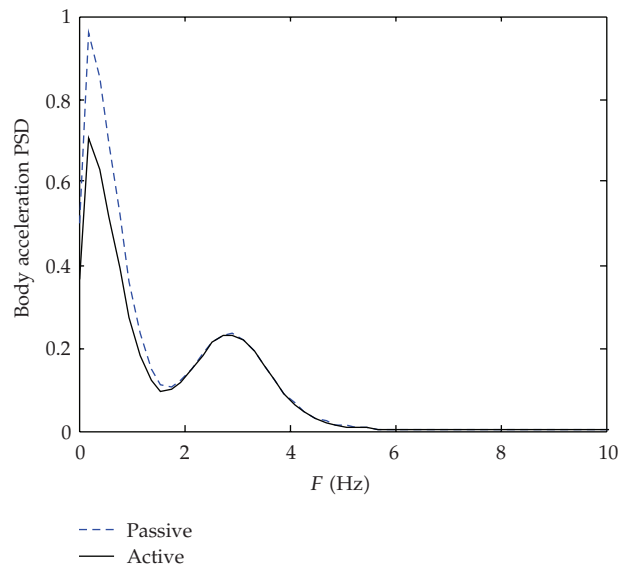


Figure 14: Power spectral density of BA.

4.6. Time Response of the Two Different Systems in Discrete Event Road Excitation

It can be seen that, from Figures 17, 18, 19, and 20, the body acceleration, pitch angle acceleration, right front axle working space and left rear wheel dynamic deflection of the active suspension have improved noticeably, the amplitudes of performance indexes become small and the oscillation time are very short in contrast with the passive suspension.

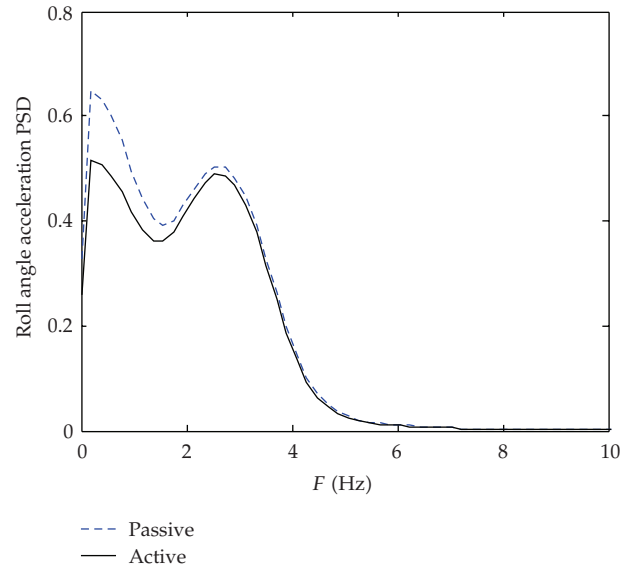


Figure 15: Power spectral density of RA.

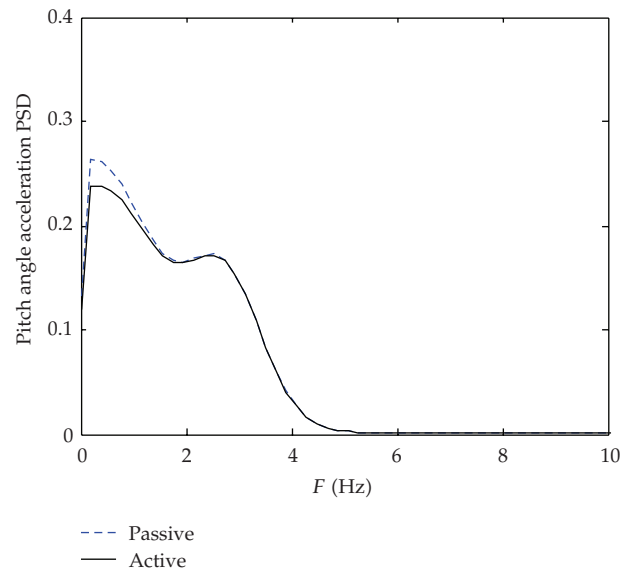


Figure 16: Power spectral density of PA.

5. Conclusion

This paper applies the optimal control theory to design a Linear Quadratic Gaussian controller for the active suspension. Especially, the methodology of AHP is used to make the selection of weighted coefficients of performance indexes, which can reduce ineffective job in contrast with experience method. From the simulation results, it can be seen that ride quality of the vehicle with active suspension has been effectively improved in comparison with the

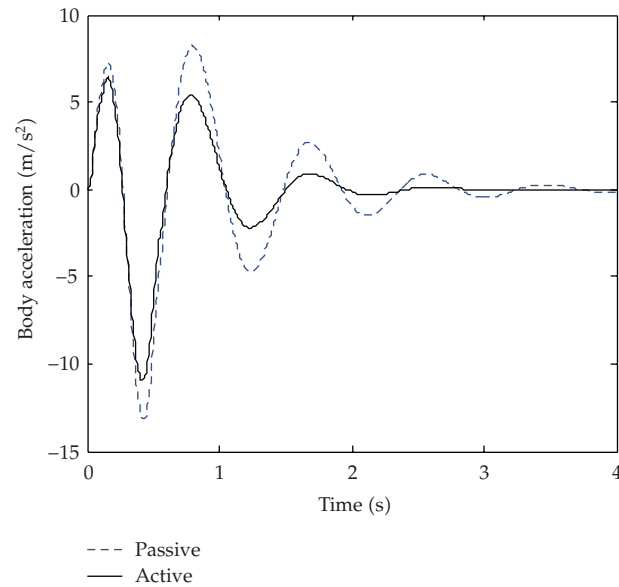


Figure 17: Body acceleration.

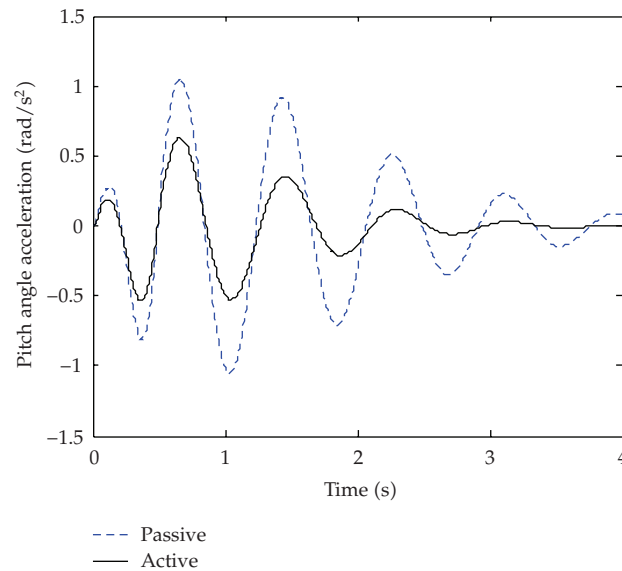


Figure 18: Pitch angle acceleration.

vehicle of passive suspension. At the same time, it can also illustrate that active suspension control system based on AHP to select weighted coefficients of the LQG controller has a good stability when suspension damping coefficients and stiffness parameters vary. Furthermore, the future work will apply AHP to investigate stability of the integrated control system that consists of an active control of vehicle suspension and a steering system in cornering on curved by means of the optimal control theory.

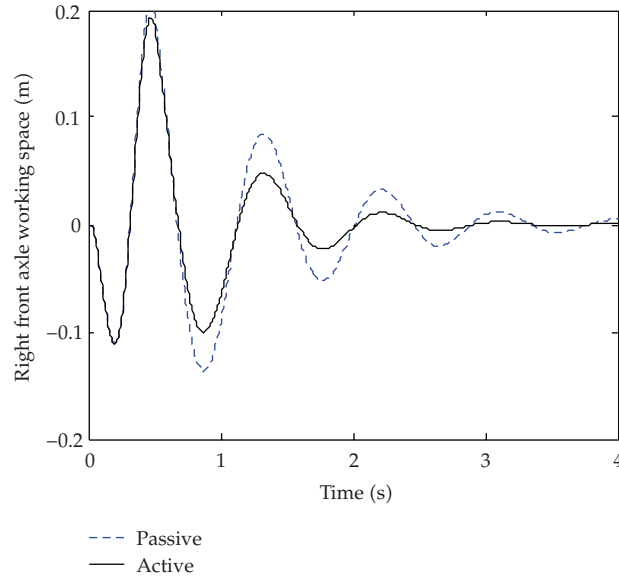


Figure 19: Right front axle working space.

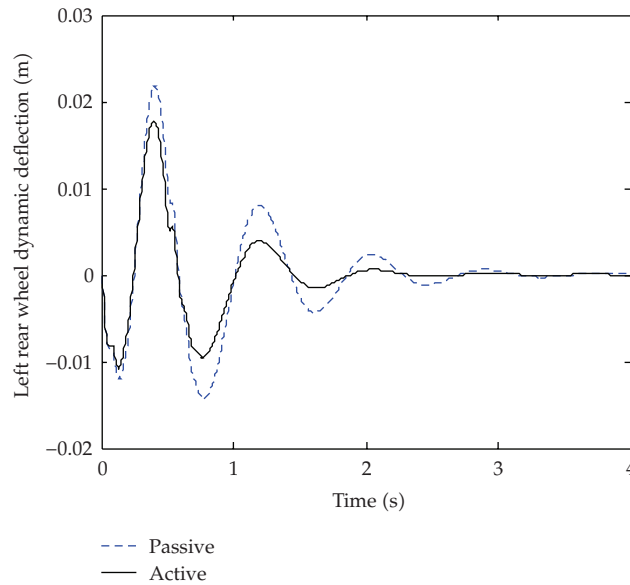


Figure 20: Left rear wheel dynamic deflection.

Acknowledgments

The authors are grateful for the support by the Shanghai Municipal Natural Science Foundation (Grant no. 10ZR1421000) and Innovation Program of Shanghai Municipal Education Commission under Grant no. 08YZ99. This paper is also supported by Shanghai Leading Academic Discipline Project of Shanghai Municipal Education Commission, project number: J50503.

References

- [1] D. Hrovat, "Survey of advanced suspension developments and related optimal control applications," *Automatica*, vol. 33, no. 10, pp. 1781–1817, 1997.
- [2] M. V. C. Rao and V. Prahlad, "A tunable fuzzy logic controller for vehicle-active suspension systems," *Fuzzy Sets and Systems*, vol. 85, no. 1, pp. 11–21, 1997.
- [3] A. Zadeh, A. Fahim, and M. El-Gindy, "Neural networks and fuzzy logic application to vehicle system," *International Journal of Vehicle Design*, vol. 18, no. 2, pp. 132–193, 1997.
- [4] S. Yun and W. Guangqiang, "Study on optimal of complete vehicle model with 7 degrees of freedom active suspension," *Automobile Technology*, vol. 6, 2007.
- [5] L. Bo and Y. Fan, "Design and simulation analysis of LQG controller of active suspension," *Transactions of the Chinese Society of Agricultural Machinery*, vol. 35, no. 1, 2004.
- [6] S.-A. Chen, F. Qiu, R. He, and S.-L. Lu, "Method for choosing weights in a suspension LQG control," *Journal of Vibration and Shock*, vol. 27, no. 2, pp. 65–68, 2008.
- [7] Z. Heng and L. Shifu, "Vehicle's time domain model with road input on four Wheels," *Automotive Engineering*, vol. 21, no. 2, 1999.
- [8] T. Runhua, C. Ying, and L. Yongxiang, "The mathematical models in time domain for the road disturbances and the simulation," *China Journal of Highway and Transport*, vol. 11, no. 3, 1998.
- [9] T. L. Saaty, *The Analytic Hierarchy Process*, McGraw Hill, New York, NY, USA, 1980.
- [10] T. Xiao and Y. Shihua, "Method of comparison matrix consistency adjustment based on AHP," *Ordnance Industry Automation*, vol. 27, no. 4, 2008.
- [11] D. Bo, "A study on optimal control for vehicle active suspension system using a whole vehicle model," *Automotive Engineering*, vol. 24, no. 24, pp. 422–425, 2002.